

Elastic Modulus Versus Bond Length in Lanthanum Chromite Ceramics

Charles S. Montross

Advanced Ceramic Development Center, University of Queensland

(Received 8 December 1994; accepted 3 July 1997)

Abstract

The elastic moduli of both oxidized and reduced MgO, CaO, and SrO doped lanthanum chromites were measured by the dynamic Young's Modulus method. The elastic modulus was also measured as a function of CaO content in both the oxidized and reduced states. From Reitveld fitting of the X-ray diffraction data, corresponding cation to anion atomic distances were calculated and compared. Changes in the elastic modulus corresponded to changes in the Cr^{+3} to O^{-2} average interatomic distance for the dopants used. © 1998 Published by Elsevier Science Limited.

1 Introduction

Lanthanum chromite ceramics form an indispensable part of solid oxide fuel cells (SOFCs) due to both high electronic conductivity and their resistance to both oxidizing and reducing conditions.¹ Often the material is used to connect cells and to separate the oxidizing air side from the hydrogen fuel side. Research into lanthanum chromites has primarily been concerned with their electrochemical behaviour versus oxygen partial pressures and dopants.

Lanthanum chromite is a perovskite ABO_3 ceramic with lanthanum on the A site and chromium on the B site. The oxygen ions surround the chromium ion to form octahedra connected at the corners by oxygen ions. The lanthanum ion is situated in a 12 fold co-ordination site between the octahedra. It had been stated that the behaviour of the octahedra determines the behaviour of the perovskite material.^{2,3}

Magnesium is used to dope the chromium B site while calcium and strontium are used to dope the lanthanum A site. Due to electroneutrality

requirements, the chromium ions change valence from +3 to +4 to compensate for the +2 valence of the alkali earths when they sit in the +3 A and B sites under oxidizing conditions. This change in valence accounts for the high electronic conductivity. The change in valence of the chromium ion also results in a change in ionic radii, from $r(+3) = 0.0615$ nm to $r(+4) = 0.055$ nm.⁴

Accurate values of the elastic modulus of lanthanum chromites would be invaluable for the analysis and design of SOFC components but there is little information noted in the literature. In the analysis by Stolten *et al.*⁵ on possible thermal stresses in SOFCs, a value of 200 GPa was used as the elastic modulus for the interconnector material. No indication was given as to the method of measurement for the elastic modulus nor for the composition of the interconnector material.

The purpose of this paper is to present the elastic modulus of both oxidized and reduced lanthanum chromites versus alkali earth dopant. The effect of varying the calcia concentration on the elastic modulus was also investigated. The crystal structure was investigated to identify possible correlations between atomic positions and elastic modulus.

2 Experimental Procedure

Commercially available magnesium doped and strontium doped lanthanum chromite powders* were used, with the chemical compositions of $La(Cr_{1-x}Mg_x)O_3$ where $x = 0.1$, and $(La_{1-x}Sr_x)CrO_3$ where $x = 0.15$, according to the provided chemical analysis. These powders were milled 24 h in isopropanol with binder and dispersant, dried, then uniaxially pressed at 70 MPa into 50 mm diameter disks. The disks were then cold isostatically pressed to 180 MPa.

After binder burnout at 600°C in air, the disks were sintered at 1700°C for 1 h under

flowing argon in a graphite element electric furnace, then cooled at greater than $200^{\circ}\text{C h}^{-1}$ to room temperature to produce the as-fired samples. The partial oxygen pressure around the samples was estimated to be $P_{\text{O}_2} = 10^{-17}$ based on Ellingham diagrams⁶ where the argon gas was deoxygenated as it flowed into and through the graphite insulation toward the samples. Other disks, after sintering under similar conditions, were subsequently heated at $200^{\circ}\text{C h}^{-1}$ to 1300°C in air, held at that temperature for 100 h, then cooled to room temperature to produce the oxidized samples.

All disks after sintering were ground flat and parallel to remove the external layer that experienced any chromium evaporation. The ground disks were lapped, then cut into bars approximately $3\text{ mm} \times 3\text{ mm}$ with lengths greater than 25 mm. The bars were polished through 1000 mesh SiC lengthwise. Flaw free bars were selected for the elastic modulus measurements.

The three chromium deficient compositions with varying calcium contents, where $x = 0.15, 0.2$ and 0.3 in $\text{La}_{1-x}\text{Ca}_x\text{Cr}_{0.97}\text{O}_3$, were prepared by the ceramic method using reagent grade La_2O_3 , Cr_2O_3 , and CaCO_3 powders. These powders were milled in isopropanol for 24 h, then calcined at 1000°C for 5 h. This was repeated for a second time. After the final calcination, the powders were milled 24 h in isopropanol with binder and dispersant, dried, then made into disks as described above. After binder burnout, disks were sintered at 1600°C for 5 h in air, then cooled at $200^{\circ}\text{C h}^{-1}$ to room temperature. The disks were ground flat and parallel to remove the external layer that experienced chromium evaporation, then made into bars as previously described.

Selected bars of all three calcium doped compositions were placed in a tube furnace for reduction by wet hydrogen with a partial oxygen pressure of $P_{\text{O}_2} = 10^{-17}$. After clearing the system of air, dry hydrogen was bubbled through 10°C water to humidify it, then through the tube furnace. The temperature was slowly ramped up to 1000°C , held at temperature for 100 h, then slowly ramped down.

The Young's Modulus measurements were performed at 25°C with a GrindoSonic system of J. W. Lemmings, Inc. by impulse excitation of vibration of the bars. The resonant frequencies were measured twice for each specimen, across the thickness and across the width. The dynamic Young's Modulus was calculated assuming a Poissons Ratio of $\nu = 0.3$ with the equations in ASTM C1259-94. One specimen per composition and condition were used.

Oxidized and reduced specimens were ground through 325 mesh then analyzed by X-ray diffraction

from 20° to $110^{\circ} 2\theta$ using $\text{Cu K}\alpha_1$ radiation with a graphite monochromator. The X-ray diffraction data for the ground powder specimens were analyzed with the Reitveld Method of analysis⁷ using the orthorhombic Pbnm space group as reported by Khattak and Cox.⁸ From the atomic positions, the bond lengths between the cations and anions were calculated.

Microprobe analyses were conducted with a 15 kV accelerating voltage on the magnesium, strontium, and calcium doped lanthanum chromites to verify compositions. Metallographic analyses of polished surfaces were also conducted to verify the density and investigate the microstructural homogeneity of the sintered specimens. After preparation of the bars, the densities were measured and the elastic moduli were corrected for porosity.⁹

3 Results

The typical microstructures for magnesium, calcium, and strontium doped lanthanum chromites are shown in Figs 1–5. The measured porosities are presented in Table 1. The magnesium doped lanthanum chromite shows a finely dispersed porosity while the calcium doped lanthanum chromite has a coarse interconnected porosity. The calcium doped material consolidates by liquid phase sintering,¹⁰ which can also cause grain coarsening, as can be seen in the figures. Strontium doped lanthanum chromite did not densify beyond the initial green density during sintering. This poor sinterability has been noted previously.

From the microprobe analysis, it was found that the microstructures of all the sintered compositions were chemically inhomogeneous. When seen through the scanning electron microscope microprobe, the microstructures were typically a mix of a light matrix, consisting primarily of lanthanum, chromium, and dopant, interspersed with a dark phase. For the calcium doped materials, the dark phase was calcium rich with lower amounts of lanthanum and chromium. This is in agreement with the liquid phase sintering mechanism for calcium doped, chromium deficient lanthanum chromite.¹⁰ In the two commercial ceramic powders, the magnesium doped and strontium doped lanthanum chromites, the dark phase contained minor contaminants such as Si or Fe. Additionally, the strontium doped lanthanum chromite contained less strontium, at approximately $x = 0.1$, than the $x = 0.15$ listed in the manufacturers chemical analysis. The result is the orthorhombic phase identified by X-ray diffraction instead of the rhombohedral phase which is normally found for

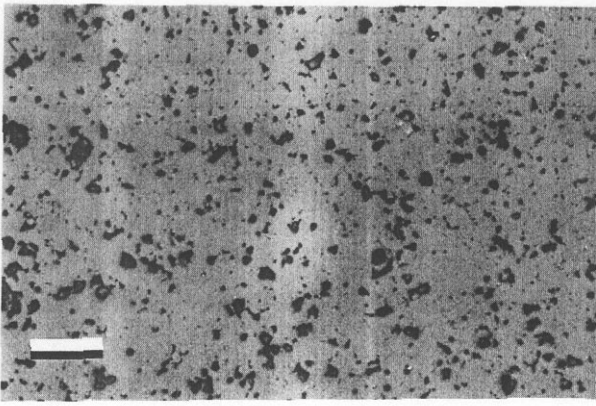


Fig. 1. Typical microstructure of $\text{La}(\text{Cr}_{1-x}\text{Mg}_x)\text{O}_3$ with the bar equal to $20\ \mu\text{m}$.

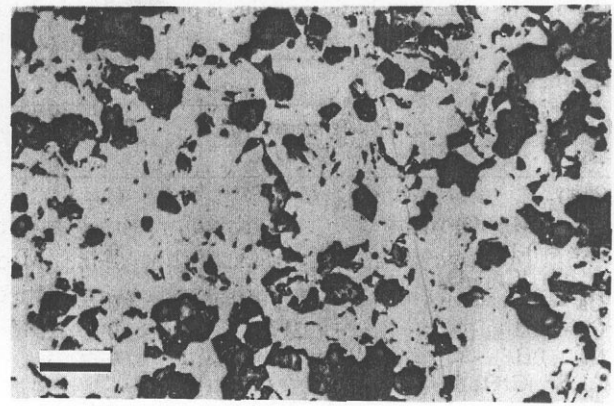


Fig. 2. Typical microstructure of $(\text{La}_{1-x}\text{Ca}_x)\text{Cr}_{0.97}\text{O}_3$, $x = 0.15$, with the bar equal to $20\ \mu\text{m}$.

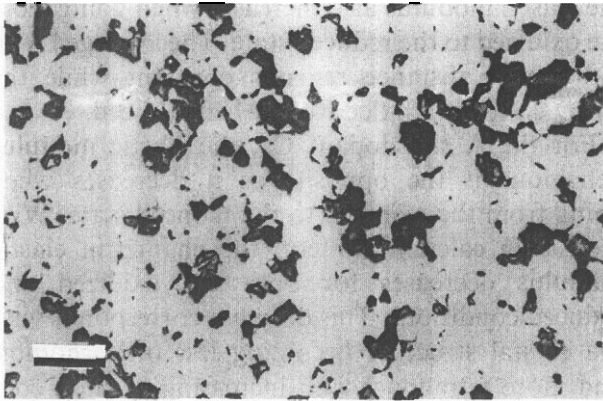


Fig. 3. Typical microstructure of $(\text{La}_{1-x}\text{Ca}_x)\text{Cr}_{0.97}\text{O}_3$, $x = 0.2$, with the bar equal to $20\ \mu\text{m}$.

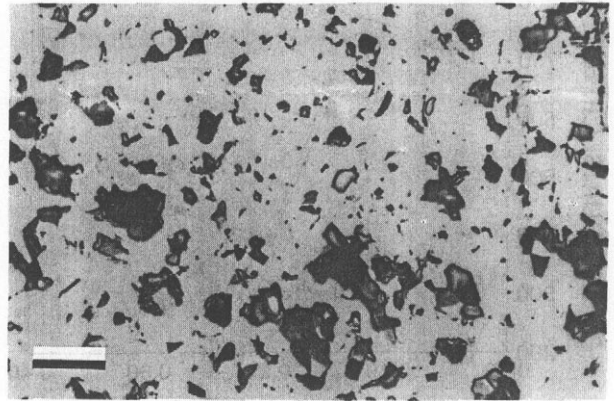


Fig. 4. Typical microstructure of $(\text{La}_{1-x}\text{Ca}_x)\text{Cr}_{0.97}\text{O}_3$, $x = 0.3$, with the bar equal to $20\ \mu\text{m}$.

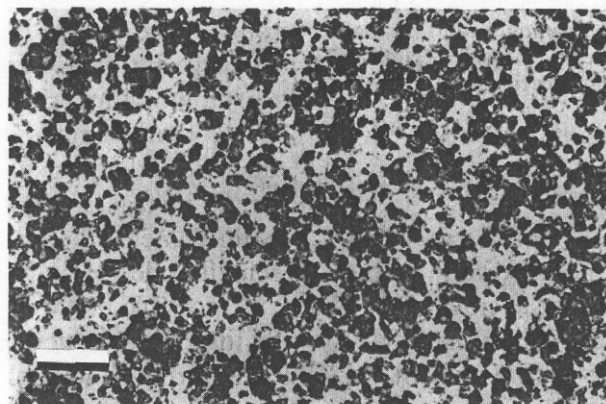


Fig. 5. Typical microstructure of $(\text{La}_{1-x}\text{Sr}_x)\text{CrO}_3$ with the bar equal to $20\ \mu\text{m}$.

compositions of higher strontium content such as $x = 0.15$.

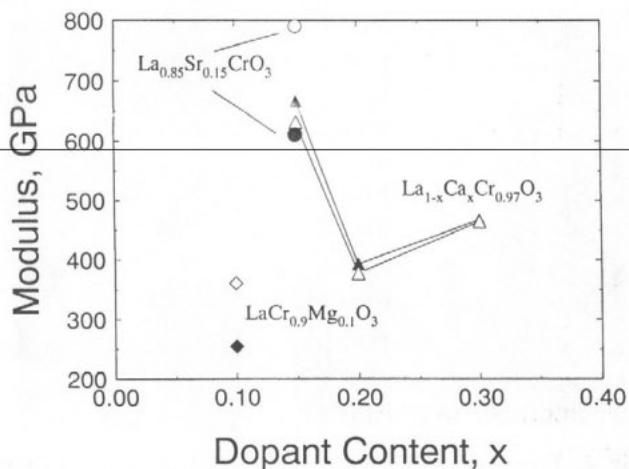
The elastic moduli were measured across the width and the thickness for each specimen and the average value was calculated. There was no significant difference between the elastic modulus measured across the width and the thickness. The as-measured and corrected average elastic modulus for each composition in both the oxidized and reduced states are shown in Table 1 with their corresponding porosity. In Fig. 6, the elastic modulus,

in GPa, is plotted against dopant content for oxidized and reduced conditions. The elastic moduli of the oxidized specimens are shown with black symbols while the elastic moduli of the reduced specimens are shown with open symbols.

From the Reitveld analysis the atomic positions were used to calculate the average La–O interatomic distances and average Cr–O bond lengths. These values are shown in Table 2 for both the oxidized and reduced states with their corresponding corrected elastic modulus.

Table 1. The corrected elastic modulus is presented, calculated from the measured elastic modulus, GPa, and measured porosity of the samples

Dopant content	Oxidized			Reduced		
	As-measured E (GPa)	Porosity	Corrected E (GPa)	As-measured E (GPa)	Porosity	Corrected E (GPa)
LaCrO ₃	—	—	—	—	—	—
La(Cr _{1-x} Mg _x)O ₃ Mg = 0.1	155.7	0.12	255	220.8	0.12	361
La _{1-x} Ca _x Cr _{0.97} O ₃ Ca = 0.15	217.6	0.28	667	206.3	0.28	632
Ca = 0.2	219.3	0.15	393	210.9	0.15	378
Ca = 0.3	187.9	0.23	468	186.8	0.23	465
La _{1-x} Sr _x CrO ₃ Sr = 0.15	93.3	0.47	611	120.7	0.47	791

**Fig. 6.** Elastic Modulus versus composition and concentration for alkali earth doped lanthanum chromite. The black symbols are measured values from oxidized specimens while the white symbols are from reduced specimens. Diamonds are for magnesia doped specimens, triangles for calcia doped specimens, and circles for strontia doped specimens.

4 Discussion

For the B site dopant Mg, the elastic modulus increases when going from the oxidized to the reduced state. Concurrently, the average La–O interatomic distance decreases while the Cr–O bond length increases. For the A site dopant Sr,

the elastic modulus also increases when going from the oxidized to the reduced state. The average La–O interatomic distance remains constant while the Cr–O bond length decreases when reduced.

For the A site dopant Ca, the elastic modulus behaviour is the opposite as it decreases when going from the oxidized to the reduced state. With increasing calcium content, the change in elastic modulus decreases for both the oxidized and reduced conditions. This decrease corresponds with the crystal structure becoming less orthorhombic and more tetragonal with increasing calcium content.^{11,12} Additionally, the magnitude of the change in elastic modulus is noticeably less than for the other two dopants.

Concurrently, both the average La–O interatomic distance and the Cr–O bond length increase when going from oxidized to reduced states. The elastic modulus primarily follows the behaviour of Cr–O bond lengths versus composition for both the oxidized and reduced states. As the Cr–O bond length increases then decreases with increasing calcium content, the elastic modulus behaves conversely, first decreasing then increasing.

A possible method of understanding the relation of the crystal structure to the elastic modulus is by considering the behaviour of the octahedral

Table 2. Mean bond lengths, nm, between cation and anions in lanthanum chromites with their respective elastic modulus, GPa. Calculated for both oxidized and reduced conditions from Reitveld analysis of X-ray diffraction data

Dopant content	Oxidized			Reduced		
	La–O (nm)	Cr–O (nm)	E (GPa)	La–O (nm)	Cr–O (nm)	E (GPa)
LaCrO ₃	0.2757	0.1970	—	—	—	—
La(Cr _{1-x} Mg _x)O ₃ Mg = 0.1	0.2756	0.1978	254	0.2744	0.2002	361
La _{1-x} Ca _x Cr _{0.97} O ₃ Ca = 0.15	0.2744	0.1958	667	0.2759	0.1967	632
Ca = 0.2	0.2744	0.1964	393	0.2761	0.1979	378
Ca = 0.3	0.2736	0.1955	468	0.2749	0.1959	465
La _{1-x} Sr _x CrO ₃ Sr = 0.15	0.2765	0.2003	611	0.2765	0.1980	791

units.^{2,3} The perovskite structure is typically depicted with octahedra connected at the corners surrounding the A site ions as shown in Fig. 7. The individual octahedra can be considered to act as a unit which when connected together form a lattice network. The degree of flexure and rotation of the octahedra with respect to each other will control the elastic modulus.

The effect of the Cr–O bond length on the elastic modulus depends upon the dopant. For A site dopants, Ca and Sr, as the Cr–O bond length decreases the elastic modulus increases. For the B site dopant, Mg, the opposite is true whereas the Cr–O bond length increases during reduction, the elastic modulus increases.

This structural behaviour can be seen by looking at the average interatomic distances and bond lengths. From Shannon, the effective ionic radii for La +3 is 0.136 nm and O^{–2} is 0.140 nm. Considering these two ions as spheres, the interatomic distance would be 0.276 nm. This value is very close to the average interatomic distances measured in this work which range from 0.274 to 0.277 nm. The variations in the lanthanum oxygen interatomic distance can be considered inconsequential.

Under reducing conditions, the effective ionic radii for Cr+3 in lanthanum chromite is 0.0615 nm. Assuming the chromium and oxygen ions act as spheres, the expected Cr–O bond length would be 0.215 nm. The measured bond lengths for reduced calcium and strontium doped lanthanum chromites are 0.198 to 0.196 nm which indicates a degree of covalent bonding. This then indicates that the octahedra will act as a unit during distortions of the crystal lattice.

The Cr–O bond is affected by changes in valence due to the electroneutrality requirements of the crystal lattice. For example, in calcium doped lanthanum chromite, for each Ca +2 ion on the La +3 site, a chromium ion must change valence from +3

to +4 under oxidizing conditions. The radius of the Cr+4 ion is 0.055 nm and by the rule of mixtures, the average bond length is calculated to be 0.2005 nm for a calcium content of $x = 0.15$. The average measured bond length is 0.1958 nm. When the calcium content is $x = 0.3$, the calculated bond length is 0.1996 nm while the measured value is 0.1955 nm. This indicates that under oxidizing conditions, the chromium to oxygen bonds also have a degree of covalent bonding.

Under reducing conditions, the relationship between elastic modulus and dopants used can be considered due to the changes in the average ionic size of the A and B site ions. In the A sites the La +3 ($r = 0.136$ nm) plus the bigger Sr +2 ($r = 0.144$ nm) ion yield an average ion ($r = 0.137$ nm) slightly bigger, resulting in a higher modulus. When Ca +2 is used at approximately the same concentration, with a radius of $r = 0.134$ nm which is slightly smaller than the La +3, the resulting average ionic size ($r = 0.1357$ nm) and elastic modulus is lower. With increasing Ca +2 content, the average ionic size decreases also resulting in a decrease in elastic modulus. When the calcia content is $x = 0.3$, the average ionic size is calculated to be $r = 0.135$ nm. The increase in elastic modulus when the calcia content is $x = 0.3$ can be considered due to the increasing tetragonality of the crystal structure.

On the B site, the relationship is also controlled by the chromium to oxygen bond length. The addition of the Mg +2 ion with $r = 0.072$ nm to the Cr +3 ion ($r = 0.0615$ nm) results in an average ionic size of $r = 0.0631$ nm and calculated bond length of 0.2031 nm. The measured value of 0.2002 nm is significantly bigger than for the other dopants. The result of the biggest bond length is the lowest measured elastic modulus of 254 to 361 MPa for oxidized and reduced conditions.

5 Conclusions

From the results presented, the following conclusions can be made.

1. The elastic modulus varied with composition and oxidation state. For magnesium and strontium doped lanthanum chromite, the elastic moduli of the oxidized specimens were lower than for the reduced specimens. For calcium doped lanthanum chromite, the elastic moduli behaved conversely where the oxidized specimens had a slightly higher elastic modulus. With increasing calcium content, the difference in elastic modulus decreased between the oxidized and reduced specimens.

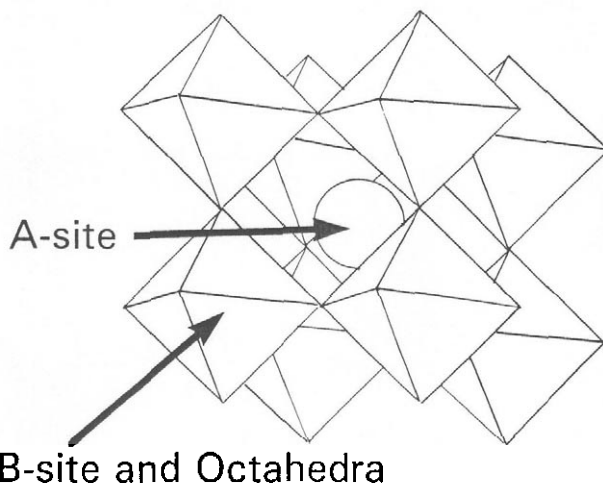


Fig. 7. Typical presentation of the perovskite structure showing the B site based octahedra surrounding the A site ion.

2. The changes in elastic modulus are related to changes in the interatomic distance between the chromium and oxygen ions. With decreasing Cr–O interatomic distance, the elastic modulus increases. The La–O interatomic distance varied slightly with oxidation state and dopant but is considered insignificant.
3. Looking at the polyhedra in the unit cell, the chromium-oxygen octahedra connected by their corners surround the lanthanum ion forming a lattice network. As the Cr–O interatomic distance decreases, the chromium octahedra which surround the La ion move in tighter, resulting in a higher elastic modulus.
4. The measured cation to anion distances support this explanation. The measured La–O interatomic distances are equivalent to the summed radii assuming the ions to be spheres. The Cr–O bond length is less than the summed effective ionic radii which indicates a degree of covalent bonding and that the octahedra will act as a unit forming the lattice network surrounding the lanthanum ion.

Acknowledgements

Dr Andre Van Leuven of J. W. Lemmens, Inc. is thanked for his help with the elastic modulus measurements. The author would also like to acknowledge Professor Wayne Dollase, Department of Earth and Space Sciences, UCLA, for his kind help with the calculations of the bond lengths and angles. Ron Rasch from the Center for Microscopy and Microanalysis, University of Queensland, Australia is thanked for the microprobe analyses of the lanthanum chromite specimens. The author would like to acknowledge the assistance in the X-ray diffraction of some of the materials by Mr Lambert Bekessy of the Department of Mining and Metallurgical Engineering, University of Queensland, Australia. The interest

of Dr Dokiya, currently at Yokohama National University, Japan is greatly appreciated. The lanthanum chromite samples were prepared during the tenure under a research fellowship provided by the Science and Technology Agency of Japan and through the R&D program of the New Sunshine Project of the Agency of Industrial Science and Technology of Japan (Ministry of International Trade and Industry). Their support is greatly appreciated.

References

1. Anderson, H. U., Review of p-type perovskite materials for SOFC and other applications. *Solid State Ionics*, 1992, **52**, 33–41.
2. Glazer, A. M., The classification of tilted octahedra in perovskites. *Acta Cryst.*, 1972, **B28**, 3384–3392.
3. Glazer, A. M., Simple ways of determining perovskite structures. *Acta Cryst.*, 1975, **A31**, 756–762.
4. Shannon, R. D., Revised effective ionic radii and systematic studies of interatomic distances in halides and chalcogenides. *Acta Cryst.*, 1976, **A32**, 751–767.
5. Stolten, D., Monreal, E. and Müller, W., *Improvement of the Mechanical Integrity of Planar SOFC Stacks*. 1992 Fuel Cell Seminar, Organizing Committee: Courtesy Associates Inc., Washington, DC, pp. 253–256.
6. Gaskell, D. R., *Introduction to Metallurgical Thermodynamics*, 2nd edn. McGraw Hill Publishers, New York, 1981, p. 287.
7. Hill, R. J. and Howard, C. J., *A computer program for Reitveld analysis of fixed wavelength X-ray and neutron powder diffraction patterns*. Australian Atomic Energy Commission Report No. M112.
8. Khattak, C. P. and Cox, D. E., Structural studies of the (La,Sr)CrO₃ system. *Mat. Res. Bull.*, 1977, **12**, 463–472.
9. Porter, D. F., Reed, J. S. and Lewis, D., Elastic modulus of refractory spinels. *J. Am. Cer. Soc.*, 1977, **60**(7–8), 345–349.
10. Sakai, N., Kawada, T., Yokokawa, H., Dokiya, M. and Iwata, T., Liquid-phase-assisted sintering of calcium-doped lanthanum chromites. *J. Am. Cer. Soc.*, 1993, **76**(3), 609–616.
11. Berjoan, R., Romand, C. and Coutures, J. C., Oxygen reactivity of La₂O₃-Cr₂O₃-CaO MHD-related materials. *High Temperature Science*, 1980, **13**, 173–188.
12. Berjoan, R. and Coutures, J., Etudes structurales du système (La, Ca) CrO₃ à température. *Rev. Int. Hautes Tempér. Réfract. Fr.*, 1980, **17**, 261–268.